5704 *Inorg. Chem.* **2009**, *48*, 5704–5714
DOI: 10.1021/ic802361q

Inorganic Chemistry
Article

Photophysical Characteristics and Reactivity of Bis(2,9-di-*tert*-butyl-1,10-phenanthroline) copper(I)

Omar Green, Bhavesh A. Gandhi, and Judith N. Burstyn*

Department of Chemistry, University of Wisconsin, Madison, Wisconsin 53706

Received December 10, 2008

The recently synthesized sterically constrained copper(I) complex $[Cu(\mathbf{dtbp})_2]^+$ (**1**), where **dtbp** is 2,9-di-*tert*-butyl-1,10-phenanthroline, exhibits unique photophysical and reactivity properties. Complex **1** (λ_{abs}, 425 nm; ε, 3100 L M^{-1} cm^{-1}; $\lambda_{emission}$, 599 nm) has the longest metal-to-ligand charge-transfer (MLCT) emission lifetime (τ, 3260 ns) and largest quantum yield (ϕ, 5.6%) of all $[Cu(R_2phen)_2]^+$ complexes. Complex **1** also exhibits a large positive reduction potential for the $[Cu^{2+}(\mathbf{dtbp})_2]$|$[Cu^{+}(\mathbf{dtbp})_2]$ couple ($E_{1/2}$ = 0.70 V vs $Fc^{+/0}$) and a large negative excited-state reduction potential for the $[Cu^{2+}(\mathbf{dtbp})(\mathbf{dtbp}^{-\bullet})]$|$[Cu^{2+}(\mathbf{dtbp})_2]$ couple ($E_{1/2}$ = −1.66 V vs $Fc^{+/0}$), indicating that this complex is a potent photoreductant in the excited state. The steric constraint imposed by the *t*-butyl substituents in **1** enables unusual ligand replacement reactivity. Either CH_3CN or CO replaces one of the **dtbp** ligands, a reaction that is readily followed by loss of the unique emission signature of **1**. Monodentate CH_3CN binds to the copper(I) center with an affinity 2 orders of magnitude greater than that of the displaced **dtbp**, despite the fact that the displaced ligand is bidentate. CO-induced displacement of **dtbp** from **1** is reversible, but only in the presence of 1 equiv of unbound **dtbp**. The exceptionally strong donor ligand CH_3NC displaces both **dtbp** ligands from **1**. In contrast to the facile ligand displacement reactivity with good donor ligands, **1** does not react readily with O_2, by either a ligand displacement or an oxidative pathway. Rather, O_2 induces partial quenching of emission via an outer-sphere interaction with **1**.

Introduction

Luminescent transition metal complexes are useful in sensors, in solid-state lighting devices, and in dye-sensitized solar energy conversion devices.[1−3] In these contexts, diimine-ligated ruthenium(II) complexes are the most commonly used compounds. There are major disadvantages to these metals in practical applications: they are rare, expensive, and toxic. Because of these drawbacks there is interest in developing luminescent complexes of the abundant, cheap, and non-toxic metal, copper.[4−6] Copper-functionalized dye-sensitized solar cells, employing diimine-copper(I) complexes as dyes, are remarkably efficient.[7] Phenanthroline-ligated copper(I) complexes are potentially useful dye candidates, as their photophysical properties may be tailored through geometric and electronic control.[5,6,8,9] In this paper we present the characterization of a homoleptic phenanthroline complex of copper(I) with photophysical properties comparable to those of tris(bipyridyl)ruthenium(II), $[Ru(bpy)_3]^{2+}$, a complex commonly applied in device design.

In phenanthroline-copper(I) complexes, metal-to-ligand charge transfer excitation formally oxidizes the copper(I) ion to copper(II), and relaxation may occur through non-emissive geometric reorganization or by radiative decay.[5,6,8,9] For copper complexes to be useful in photochemical devices, the tendency of copper to undergo geometric reorganization toward square planar geometry on excitation must be inhibited to maximize the radiative decay of the excited state. Copper(I) complexes that meet this requirement include the homoleptic $[Cu(R_2Phen)_2]^+$ complexes, where R_2Phen is a 2,9-disubstituted phenanthroline.[10] Substitution at the 2 and 9 positions, those closest to the copper(I) ion, inhibit the geometric reorganization and thus maximize radiative emission.[5,6,9] The first example of room temperature emission from this class of complexes was reported by Blaskie and

*To whom correspondence should be addressed. E-mail: burstyn@chem.wisc.edu. Phone: 608-262-0328. Fax: 608-262-6143.

(1) Rogers, C. W.; Wolf, M. O. *Coord. Chem. Rev.* **2002** 233–234, 341−350.
(2) O'Regan, B.; Graetzel, M. *Nature (London)* **1991**, *353*, 737–40.
(3) Evans, R. C.; Douglas, P.; Winscom, C. J. *Coord. Chem. Rev.* **2006**, *250*, 2093–2126.
(4) Barbieri, A.; Accorsi, G.; Armaroli, N. *Chem. Commun.* **2008** 2185–2193.
(5) Lavie-Cambot, A.; Cantuel, M.; Leydet, Y.; Jonusauskas, G.; Bassani, D. M.; McClenaghan, N. D. *Coord. Chem. Rev.* **2008**, *252*, 2572–2584.
(6) Armaroli, N.; Accorsi, G.; Cardinali, F.; Listorti, A. *Top. Curr. Chem.* **2007**, *280*, 69–115.
(7) Bessho, T.; Constable, E. C.; Graetzel, M.; Hernandez Redondo, A.; Housecroft, C. E.; Kylberg, W.; Nazeeruddin, M. K.; Neuberger, M.; Schaffner, S. *Chem. Commun.* **2008**, 3717–3719.
(8) Armaroli, N. *Chem. Soc. Rev.* **2001**, *30*, 113–124.
(9) Scaltrito, D. V.; Thompson, D. W.; O'Callaghan, J. A.; Meyer, G. J. *Coord. Chem. Rev.* **2000**, *208*, 243–266.
(10) Abbreviations used: dtbp, 2,9-di-*tert*-butyl-1,10-phenanthroline; dmp, 2,9-dimethyl-1,10-phenanthroline; dpp, 2,9-diphenyl-1,10-phenanthroline; xop, 2-(2-methylphenyl)-9-(2,6-dimethylphenyl)-1,10-phenanthroline; dnpp, 2,9-dineopentyl-1,10-phenanthroline; dipp, 2,9-di-isopropyl-1,10-phenanthroline; dbp, 2,9-butyl-1,10-phenanthroline; dsbp, 2,9-*sec*-butyl-1,10-phenanthroline; phen, 1,10-phenanthroline.

Published on Web 06/04/2009

Table 1. Photophysical Characteristics of $[Cu(R_2Phen)_2]^+$ Complexes in CH_2Cl_2 Solution and Comparison with Those of $[Ru(bpy)_3]^{+a,b}$

complex	λ_{Abs}, nm	$\varepsilon_{\lambda max}$, L mol^{-1} cm^{-1}	λ_{Em}, nm	$E_{Abs} - E_{Em}$, eV	τ, ns	$\phi_{em} \times 10^3$	$k_r 10^3$ s^{-1}	k_{nr} 10^7 s^{-1}	references
$[Ru(bpy)_3]^{2+}$	446−454	∼14000	580−630	0.617−0.799	530−1250	29−270			59
$[Cu(\mathbf{dtbp})_2]^+$	425	3100	599	0.847	3260	56	17.18	0.03	this work
$[Cu(\mathbf{dtbp})(dmp)]^+$	440	7000	646	0.899	730	10	13.70	0.14	20
$[Cu(dsbp)_2]^+$	455	6600	690	0.928	400	4.5	11.25	0.25	12
$[Cu(dipp)_2]^+$	445	7500	650	0.879	365	4.0	10.90	0.27	60
$[Cu(dnpp)_2]^+$	449	5700	715	1.027	260	1.6	6.15	0.38	12
$[Cu(dbp)_2]^+$	457	7000	725	1.003	150	0.9	6.00	0.66	12
$[Cu(dmp)_2]^+$	457	7800	730	1.015	90	0.4	4.44	1.11	12
$[Cu(dpp)_2]^+$	440	3800	690	1.021	243	0.87	3.58	0.41	19
$[Cu(bfp)_2]^+$	462	10900	665	0.819	165	3.3	20.00	0.60	42
$[Cu(xop)_2]^+$	452	3000	673	0.901	149	1.0	6.71	0.67	19

[a] The data for $[Ru(bpy)_3]^+$ are presented as a range because they were collected in a variety of solvents. [b] Abbreviations: **dtbp**, 2,9-di-*tert*-butyl-1,10-phenanthroline; dmp, 2,9-dimethyl-1,10-phenanthroline; dsbp, 2,9-*sec*-butyl-1,10-phenanthroline; dipp, 2,9-di-isopropyl-1,10-phenanthroline; dnpp, 2,9-dineopentyl-1,10-phenanthroline; dbp, 2,9-butyl-1,10-phenanthroline; xop, 2-(2-methylphenyl)-9-(2,6-dimethylphenyl)-1,10-phenanthroline; dpp, 2,9-diphenyl-1,10-phenanthroline;bfp, 2,9-bis(trifluoromethyl)-1,10-phenanthroline.

McMillin,[11] who contrasted the luminescence of $[Cu(dmp)_2]^+$ with that of non-emissive $[Cu(phen)_2]^+$. The methyl groups at the 2 and 9 positions provided sufficient steric bulk that $[Cu(dmp)_2]^+$ emitted at room temperature in CH_2Cl_2 solution.

Emission from $[Cu(dmp)_2]^+$ is characterized by a short excited-state lifetime (90 ns), a modest quantum yield (4.0×10^{-4}), and facile quenching by exogenous ligands.[12] When $[Cu(dmp)_2]^+$ distorts toward square planar geometry in the excited state, a new coordination site becomes accessible, and small molecule ligands may bind and quench the emission.[13,14] $[Cu(dmp)_2]^+$ does not emit in coordinating solvents, and addition of Lewis bases in non-coordinating solvents quenches the emission.[11] Exciplex formation through ligand binding to the flattened copper(II)-like excited state is a primary reaction path for $[Cu(dmp)_2]^+$.[13,15,16] This pathway shuts down when sufficient steric bulk is added on either the phenanthroline ligand, as in the case of 2,9-diphenyl-1,10-phenanthroline, or the incoming Lewis base, as in the case of 2,6-dimethylpyridine.[17]

Subsequent studies have shown that the photophysical properties of $[Cu(R_2Phen)_2]^+$ complexes vary with the steric demand at the 2 and 9 positions.[11,12,17−25] As the geometric reorganization of the excited state is inhibited by the addition of bulkier substituents, both the lifetime and the quantum yield increase. To date, the most sterically demanding combination of substituents was in a complex with heteroleptic ligation, $[Cu(dmp)(\mathbf{dtbp})](PF_6)$.[20] This complex exhibited the longest lifetime (730 ns) and the largest quantum yield (1×10^{-2}) among complexes with 2,9-dialkyl substituents. As illustrated in Table 1, the lifetime and quantum yield increase with increasing steric demand of the substituents because of inhibition of non-radiative vibrational relaxation. Increased ligand bulk also shuts down Lewis base-induced quenching via exciplex formation; homoleptic complexes with bulky phenanthroline ligands emit even in acetonitrile, tetrahydrofuran, or methanol solutions.[12,19]

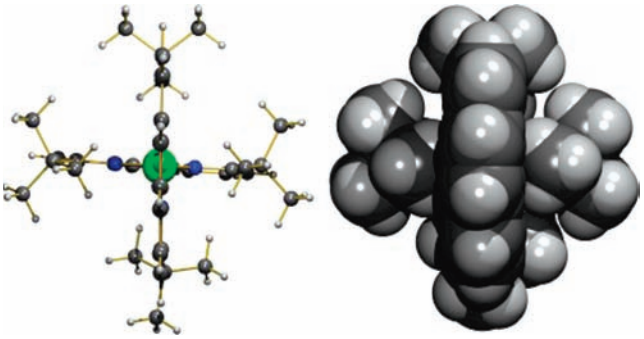

Figure 1. Ball and stick and space filling diagrams of $[Cu(\mathbf{dtbp})_2]^+$ derived from the crystallographic coordinates.[26]

Recently, we designed a strategy that enabled synthesis of $[Cu(\mathbf{dtbp})_2][B(C_6F_5)_4]$, (**1**), the most sterically encumbered homoleptic $[Cu(R_2Phen)_2]^+$ complex prepared to date.[26] As illustrated by the space filling diagram in Figure 1, the *tert*-butyl substituents impart limits on the potential for geometric reorganization in $[Cu(\mathbf{dtbp})_2]^+$. Consistent with substantial steric constraint, this complex exhibits an average copper(I)−N bond length of 2.11 Å, which is significantly longer than the 2.04 Å average copper(I)−N bond length for all other complexes in this class. We report herein photophysical characterization of **1** and exploration of the unique reactivity of **1** that is afforded by the sterically weakened copper(I)−N bonds. The reactivity of **1**, particularly the role of **dtbp** in this reactivity, is investigated by comparison with a complex

(11) Blaskie, M. W.; McMillin, D. R. *Inorg. Chem.* **1980**, *19*, 3519–3522.
(12) Eggleston, M. K.; McMillin, D. R.; Koenig, K. S.; Pallenberg, A. J. *Inorg. Chem.* **1997**, *36*, 172–176.
(13) McMillin, D. R.; Kirchhoff, J. R.; Goodwin, K. V. *Coord. Chem. Rev.* **1985**, *64*, 83–92.
(14) Chen, L. X.; Shaw, G. B.; Novozhilova, I.; Liu, T.; Jennings, G.; Attenkofer, K.; Meyer, G. J.; Coppens, P. *J. Am. Chem. Soc.* **2003**, *125*, 7022–7034.
(15) Everly, R. M.; McMillin, D. R. *J. Phys. Chem.* **1991**, *95*, 9071–9075.
(16) Stacy, E. M.; McMillin, D. R. *Inorg. Chem.* **1990**, *29*, 393–396.
(17) Dietrich-Buchecker, C. O.; Marnot, P. A.; Sauvage, J. P.; Kirchoff J. R.; McMillin, D. R. *Chem. Commun.* **1983**, 513–515.
(18) Dietrich-Buchecker, C. O.; Nierengarten, J. F.; Sauvage, J. P.; Armaroli, N.; Balzani, V.; De Cola, L. *J. Am. Chem. Soc.* **1993**, *115*, 11237–11244.
(19) Miller, M. T.; Gantzel, P. K.; Karpishin, T. B. *Inorg. Chem.* **1999**, *38*, 3414–3422.
(20) Miller, M. T.; Gantzel, P. K.; Karpishin, T. B. *J. Am. Chem. Soc.* **1999**, *121*, 4292–4293.
(21) Miller, M. T.; Gantzel, P. K.; Karpishin, T. B. *Inorg. Chem.* **1998**, *37*, 2285–2290.
(22) Cunningham, C. T.; Cunningham, K. L. H.; Michalec, J. F.; McMillin, D. R. *Inorg. Chem.* **1999**, *38*, 4388–4392.
(23) Eggleston, M. K.; Fanwick, P. E.; Pallenberg, A. J.; McMillin, D. R. *Inorg. Chem.* **1997**, *36*, 4007–4010.
(24) Felder, D.; Nierengarten, J.-F.; Barigelletti, F.; Ventura, B.; Armaroli, N. *J. Am. Chem. Soc.* **2001**, *123*, 6291–6299.
(25) Kalsani, V.; Schmittel, M.; Listorti, A.; Accorsi, G.; Armaroli, N. *Inorg. Chem.* **2006**, *45*, 2061–2067.
(26) Gandhi, B. A.; Green, O.; Burstyn, J. N. *Inorg. Chem.* **2007**, *46* 3816–3825.

that has only a single 2,9-di-*tert*-butyl-1,10-phenanthroline ligand, [Cu(**dtbp**)(acetone)](SbF_6).[26]

Experimental Section

All reagents were purchased from Aldrich Chemical Co. and purified according to literature procedures unless otherwise noted. CH_3CN, CH_2Cl_2 and *n*-hexane were purchased as spectroscopic grade (Burdick & Jackson) and distilled from CaH_2 under N_2. All solvents were further degassed by three freeze−pump−thaw cycles or by sparging with Ar. The complexes [Cu(**dtbp**)$_2$][$B(C_6F_5)_4$] (**1**), [Cu(**dtbp**)($NCCH_3$)](PF_6), [Cu(**dtbp**)(acetone)](SbF_6), and [Cu(**dtbp**)(dmp)](BF_4) were synthesized using a recently developed method, which is described elsewhere.[26] [Ru(bpy)$_3$][(PF_6)$_2$] was synthesized and purified according to literature procedure.[27] CH_3NC was synthesized as described[28] and was used immediately. O_2 (99.5%) and CO (99.5%) were purchased from BOC and AGA Gases, respectively, and were used as received. All spectra were recorded on samples that were maintained under an inert atmosphere (N_2) unless otherwise noted. Igor Pro 4.08 was used to process and fit spectrophotometric data to obtain peak positions and integrated intensities.

Spectrophotometric Measurements. Electronic absorption spectra were obtained with a Varian Cary 4 Bio spectrophotometer, and photoluminescence data were collected with an ISS PC-1 spectrofluorometer outfitted with a 300 W high pressure Xe arc lamp source. All emission spectra were corrected by applying correction factors provided with the instrumental software (Vinci; v. 0.0797, ISS Inc.), which are specific to the instrument. The quantum yield of **1** was estimated[29] using [Ru(bpy)$_3$][(PF_6)$_2$] in water as a standard ($\Phi_{em} = 0.042$).[30] The emission spectrum of **1** in degassed CH_2Cl_2 was recorded using 425 nm excitation. Igor Pro 4.08 was used to fit the corrected emission spectrum to two Gaussians and to measure the area under the curve. Integrated emission intensities were obtained for **1** at three different concentrations, with 425 nm absorbance values between 0.08 and 0.04 to avoid inner filter effects. An approximate quantum yield was calculated according to eq 1, where Q is the quantum yield, I is the integrated emission intensity, OD is the optical density, and n is the refractive index. The subscript R denotes the reference values for the standard [Ru(bpy)$_3$][(PF_6)$_2$]. The integrated emission intensity of **1** was similarly compared to that of [Cu(**dtbp**)(dmp)](BF_4).[20]

$$Q/Q_R = (I/I_R)(OD_R/OD)(n^2/n_R^2) \quad (1)$$

Emission lifetime data for **1** in CH_2Cl_2 were collected with an ISS Chronos lifetime spectrometer equipped with a 370 nm LED source. Frequency and phase-modulated data were collected with a 550 kV long pass filter. The reference standard was $Ru(bpy)_2Cl_2$. The experimental data for **1** were best fit with a single exponential decay time of 3260 ns. Radiative and nonradiative relaxation rates were calculated according to literature procedure.[9]

Electrochemical Measurements. Cyclic voltammetry to determine the redox potential of **1** was performed using a BAS Epsilon potentiostat outfitted with a glassy carbon working electrode, a Ag|AgCl reference electrode and a Pt auxiliary electrode. The electrochemical analyses were performed under an Ar atmosphere in a homemade cell designed for low volume applications.[31] The sample, a 0.1 M solution of **1** in CH_2Cl_2 with 0.1 M tetrabutylammonium hexafluorophosphate as the supporting electrolyte, was contained within a Teflon sleeve on the working electrode. Data were collected at a scan rate of 50 mV/s. The $E_{1/2}$ of the ferrocene$^{0/+}$ couple was 500 mV versus Ag|AgCl in CH_2Cl_2 under identical experimental conditions to those used for studying **1**.

Measurement of the Binding Constant for the Second dtbp Ligand in 1. The binding constant for the second **dtbp** ligand in complex **1** was determined. In this experiment, [Cu(**dtbp**)(acetone)](SbF_6) (3.6×10^{-5} M in CH_2Cl_2) was titrated with aliquots (3 μL, 0.2 equiv) of a solution of **dtbp** (4.8×10^{-3} M in CH_2Cl_2), and binding was followed by the growth of the 425 nm metal-to-ligand charge-transfer (MLCT) peak. The experiment was performed in triplicate. The binding constant at room temperature was calculated employing a method for complexes with high binding efficiency.[32]

Spectrophotometric Studies of Ligand Reactivity. The reactivity of **1** with exogenous ligands CH_3CN and CH_3NC was studied using absorption and emission spectrophotometric titrations. A solution of **1** (2 mL of a 3.6×10^{-5} M solution in CH_2Cl_2) was placed in a photoluminescence cuvette and titrated with ligand (3.6×10^{-3} M). An aliquot of the titrant (0.20 or 0.25 equiv, 4 or 5 μL, respectively) was added to the sample and reference cells, and the solutions were stirred vigorously for 5 min. After each addition, the absorption spectrum was recorded followed immediately by the photoluminescence spectrum. The binding affinities of CH_3CN and CH_3NC were calculated, from emission and absorption data independently for their respective titrations, according to the method for high binding constants.[32]

Reaction of **1** with the gaseous ligands, CO and O_2, was also followed by absorption and emission spectroscopy. In these experiments the gaseous ligands (50 μL, 31 equiv O_2, 46 equiv CO) were bubbled into a solution of **1** in CH_2Cl_2 (3.6×10^{-5} M) via a gastight syringe, after which the absorption and emission spectra were recorded. To test the reversibility of these reactions, the solution was sparged with Ar for 5 min, the lost solvent was replaced, and again absorption and emission spectra were recorded.

^{1}H NMR Studies of Ligand Reactivity. ^{1}H NMR was used to follow the reaction of **1** with CH_3CN. ^{1}H NMR spectra were obtained on a Bruker AC$^+$ 300a spectrometer at room temperature. Chemical shifts were referenced to residual deuterated solvent protons and are reported in parts per million (ppm) versus $(CH_3)_4Si$. Complex **1** (0.01 M in CD_2Cl_2) was titrated with CH_3CN (0.2 M in CD_2Cl_2) in 0.25 equiv increments. After addition of each aliquot of CH_3CN, the tube was agitated and allowed to equilibrate for 5 min before the spectrum was recorded.

FT Raman Studies of Ligand Reactivity. The reactions of **1** with CH_3CN and CO were followed by FT Raman spectroscopy. FT Raman data were collected with a RFS 100 spectrometer. A vial charged with 100 μL of 0.1 M solution of **1** in CH_2Cl_2 was titrated with 0.5 M CH_3CN in CH_2Cl_2 in 5 μL (0.25 equiv) aliquots. After each addition the solution was agitated for 5 min, and an FT Raman spectrum was recorded. To follow the reaction of **1** with CO, 100 μL aliquots of pure gaseous CO were introduced through a septum into a vial containing 100 μL of a 0.1 M solution of **1** in CH_2Cl_2. The vial

(27) Lee, K. W.; Slinker, J. D.; Gorodetsky, A. A.; Flores-Torres, S.; Abruna, H. D.; Houston, P. L.; Malliaras, G. G. *Phys. Chem. Chem. Phys.* **2003**, *5*, 2706–2709.
(28) Cappon, J. J.; Witters, K. D.; Baart, J.; Verdegem, P. J. E.; Hoek, A. C.; Luiten, R. J. H.; Raap, J.; Lugtenburg, J. *Recl. Trav. Chim. Pays-Bas* **1994**, *113*, 318–328.
(29) Lakowicz, J. R. *Principles of Fluorescence Spectroscopy*; 3rd ed.; Springer: New York, NY, 2006.
(30) Caspar, J. V.; Meyer, T. J. *J. Am. Chem. Soc.* **1983**, *105*, 5583–5590.
(31) Feinberg, B. A.; Liu, X.; Ryan, M. D.; Schejter, A.; Zhang, C.; Margoliash, E. *Biochemistry* **1998**, *37*, 13091–13101.
(32) Bourson, J.; Pouget, J.; Valeur, B. *J. Phys. Chem.* **1993**, *97* 4552–4557.

was agitated vigorously for 5 min and an FT Raman spectrum was recorded.

FT-IR Studies of Ligand Reactivity. The reactions of CO with the complexes **1** and [Cu(**dtbp**)(acetone)](SbF_6) were monitored by FT-IR spectroscopy. Spectra were obtained on a Bruker Vertex 70 spectrometer using a liquid IR cell (NaCl windows, 0.1 mm path length), into which the sample aliquot was introduced via a gastight syringe. Solutions of **1** and [Cu(**dtbp**)(acetone)](SbF_6) in CH_2Cl_2 (0.1 M) were prepared in septum-sealed vials under N_2, and the IR spectrum of an aliquot of each sample was recorded. The solutions were sparged with CO gas for approximately 5 min until the color change was complete: from yellow-orange to pale yellow in the case of **1**, and from bright to pale yellow in the case of [Cu(**dtbp**)(acetone)](SbF_6). Fresh CH_2Cl_2 was added as needed to restore the sample volume, and the spectrum of an aliquot was recorded. The solvent was then removed under vacuum, the solid was redissolved in fresh CH_2Cl_2, and the spectrum of an aliquot was recorded. To the solution that originally contained [Cu(**dtbp**)(acetone)](SbF_6) was added excess **dtbp**. This solution was then taken to dryness under vacuum, the solid was redissolved in fresh CH_2Cl_2, and the spectrum of an aliquot was recorded.

Synthesis of [Cu(dtbp)(CO)](SbF_6). CO was allowed to flow through a vial charged with a bright yellow CH_2Cl_2 solution of [Cu(**dtbp**)(acetone)](SbF_6) until the solvent completely evaporated. The resulting pale yellow solid was dissolved in fresh CH_2Cl_2, and CO was bubbled again until nothing remained but a white solid. Crystallization of this solid from CH_2Cl_2/hexanes yielded long colorless plates of [Cu(**dtbp**)(CO)](SbF_6). ^{1}H NMR (300 MHz, CD_2Cl_2): δ 1.805 (s, 18H, CH_3), δ 8.001 (s, 2H, CH), δ 8.159 (d, J = 8.4 Hz, 2H, CH), δ 8.621 (d, J = 9 Hz, 2H, CH) ppm. ^{13}C NMR (125 MHz, CD_2Cl_2) δ 34.01, 41.29, 125.66, 129.32, 130.72, 143.86, 145.95, 172.72, 173.24 ppm. IR (cm^{-1}): SbF_6^-, 654; CO, 2130.

X-ray Structure Determination for [Cu(dtbp)(CO)](SbF_6). Under the microscope, several seemingly single crystals of [Cu(**dtbp**)(CO)](SbF_6), of which none showed any optical evidence of twinning, were selected under oil in air at room temperature. All examined crystals were twinned, and the structure was solved based on the data set collected on a non-merohedrally twinned crystal using CellNow.[33,34] The twin components were related by a 179.6° rotation about the *c* axis, with the minor component contribution of 47.85%. Data frames were integrated with the Bruker SAINT-Plus software package, and unit-cell parameters were obtained from CellNow. Data were correct for absorption effects with TWINABS [μ(Mo Kα) = 2.216 mm^{-1}; max/min transmission, 0.660/0.808]. The crystal structure of [Cu(**dtbp**)(CO)](SbF_6) was solved by direct methods. All non-hydrogen atoms were identified on the initial electron density map, and refined anisotropically by full-matrix least-squares methods; all hydrogen atoms were calculated at idealized positions and then refined as riding atoms with individual isotropic coefficients. Details of the data collection and refinement are listed in Supporting Information, Table S1, and structural parameters are provided in Supporting Information, Tables S2−S6.

Results

Photophysical and Electrochemical Attributes of [Cu(dtbp)$_2$][B(C_6F_5)$_4$] (1). Photophysical Studies. The absorption spectrum, emission spectrum and excitation profile of **1** are shown in Figure 2. The absorption features are typical of bis(phenanthroline)copper(I) complexes,

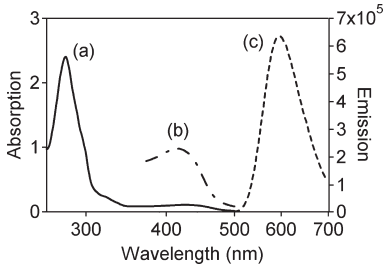

Figure 2. Absorption, excitation, and emission profiles of **1** in CH_2Cl_2. (a) The absorption spectrum exhibits intense $\pi\rightarrow\pi^*$ transition centered at 275 nm and weaker MLCT transition centered at 425 nm. (b) The excitation profile of **1** is overlaid on the absorption spectrum. Maximal emission intensity (599 nm) correlates with excitation into the MLCT absorption band. (c) The emission spectrum obtained with 425 nm excitation shows a broad emission peak centered at 599 nm.

including intense $\pi\rightarrow\pi^*$ ligand absorption (275 nm) and less intense d$\pi\rightarrow\pi^*$ MLCT absorption (425 nm).[9] The magnitude of the extinction coefficient of the MLCT transition (Table 1) is on the order expected for a d$\pi\rightarrow\pi^*$ transition.[35] Excitation into this absorption band produces a broad emission band with a maximum at 599 nm, typical of emission from an MLCT excited state.[9] The 425 nm feature is absent from the spectrum of the **dtbp** ligand, supporting the assignment of this band to the MLCT absorption in the complex.

Complex **1** exhibits the longest lifetime and highest quantum yield for this class of compounds (Table 1), substantially larger than those observed for [Cu(**dtbp**)(dmp)]$^+$.[20] MLCT-derived emission from **1** is characterized by a lifetime (τ) of 3260 ns and an estimated quantum yield (ϕ) of 5.6 (±0.4)% (5.6×10^{-2}). The improvement in the emission characteristics of **1**, relative to those of [Cu(**dtbp**)(dmp)]$^+$,[20] appears to be due to a reduction in the non-radiative relaxation rate by almost a full order of magnitude. The calculated radiative relaxation rate ($k_r = \phi/\tau$) for **1** is 1.7 (±0.2) $\times 10^4$ s^{-1}, while the non-radiative relaxation rate ($k_{nr} = (1 - \phi)/\tau$) is 3.0 (±0.2) $\times 10^5$ s^{-1}.[9] The quantum yield of **1** in CH_2Cl_2 is approximately 50% larger than that of [Ru(bpy)$_3$][(PF_6)$_2$] in water.[30] Direct comparison of the MLCT-derived emission intensity of complex **1** with that of [Cu(**dtbp**)(dmp)](BF_4), under the same solution conditions, indicates that the quantum yield of **1** is approximately five times larger (Supporting Information, Figure S1).

Electrochemical Analysis. The reduction potential of complex **1** (0.1 M) in CH_2Cl_2 solution was measured by cyclic voltammetry (Supporting Information, Figure S2). The voltammetric behavior of complex **1** was not ideal: in a single cycle the forward and reverse currents were not the same ($i_{pa}/i_{pc} = 0.75$, where i_{pa} and i_{pc} are the intensities of the anodic and cathodic peak, respectively), and the current flow in both sweep directions decreased upon a second cycle. These observations suggest that the complex degraded during the course of the experiment. Reasonable behavior was obtained at a sweep rate of 50 mV/sec. The separation of 180 mV between the anodic and cathodic peaks was within the 100−200 mV range that has been observed for others of this class of complexes.[9] The apparent

(33) *SADABS V.2.05, T., SAINT V.6.22, SHELXTL V.6.10, SMART V.5.622 Software Reference Manuals*; Bruker-AXS: Madison, WI, 2000−2004

(34) Sheldrick, G. M.; University of Göttingen: Göttingen, Germany, 2005.

(35) Harris, D. C.; Bertolucci, M. D. *Symmetry and Spectroscopy: An Introduction to Vibrational and Electronic Spectroscopy*; Dover Publications: New York, 1978.

Table 2. $Cu^{2+/+}$ Potentials of Selected $[Cu(R_2Phen)_2]^+$ Complexes and Their Derived Excited-State Reduction Potentials[a,b]

complex	$E(Cu^{2+/+})$,[c] V	ΔG_{es}, eV	$E(Cu^{2+/+*})$,[d] V	reference
$[Cu(dtbp)_2]^+$	0.70	2.36	−1.66	this work
$[Cu(dsbp)_2]^+$	0.68	2.21	−1.53	12
$[Cu(dbp)_2]^+$	0.61	2.14	−1.53	12
$[Cu(dmp)_2]^+$	0.50	2.04	−1.54	12
$[Cu(bfp)_2]^+$	1.1	2.14	−1.04	42

[a] The first four complexes are listed in order of decreasing bulk of the alkyl ligand. [b] Abbreviations: bfp, 2,9-bis(trifluoromethyl)-1,10-phenanthroline; **dtbp**, 2,9-di-*tert*-butyl-1,10-phenanthroline; dsbp, 2,9-*sec*-butyl-1,10-phenanthroline; dbp, 2,9-dibutyl-1,10-phenanthroline; dmp, 2,9-dimethyl-1,10-phenanthroline. [c] All values listed were measured versus ferrocene ($Fc^{+/0}$) in CH_2Cl_2. [d] $E(Cu^{2+/+*}) = E(Cu^{2+/+}) - \Delta G_{es}$; calculated versus ferrocene ($Fc^{+/0}$)

$E_{1/2}$ of 1200 mV vs Ag|AgCl, 700 mV vs $Fc^{+/0}$, was assigned to the $Cu^{2+/+}$ couple (Table 2).

An estimate of the reduction potential of the excited state may be calculated from the emission spectral data and the ground-state reduction potential. The maximum free energy of an emissive state (ΔG_{es}, eV) may be determined by extending a tangent from the high-energy side of the emission spectrum to the energy axis.[36] The value for ΔG_{es} of **1** obtained by use of this method and those reported for related complexes in the literature are listed in Table 2. The excited-state potential $[Cu^{2+}(R_2Phen)_2]|[Cu^{2+}(R_2Phen)(R_2Phen^{-\bullet})]$ may be estimated from ΔG_{es}, which is the maximum energy difference between photoexcited $[Cu^{2+}(R_2Phen)(R_2Phen^{-\bullet})]$ and ground $[Cu^{+}(R_2Phen)_2]$, and $E_{1/2}$, which measures the energy difference between $[Cu^{2+}(R_2Phen)_2]$ and $[Cu^{+}(R_2Phen)_2]$. The difference between $E_{1/2}$ and ΔG_{es} is then the potential for the $[Cu^{2+}(R_2Phen)_2]|[Cu^{2+}(R_2Phen)(R_2Phen^{-\bullet})]$ reduction process.[9] The excited-state reduction potential of **1** was estimated from this method to be −1.66 V versus ferrocene$^{+/0}$. A comparison of estimated potentials for the $[Cu^{2+}(R_2Phen)_2]|[Cu^{2+}(R_2Phen)(R_2Phen^{-\bullet})]$ process for **1** and related complexes is given in Table 2.

Reactivity of 1 and Related Complexes with Exogenous Ligands. Binding Affinity of the Second dtbp Ligand. Complex **1** undergoes facile ligand replacement reactions, where one **dtbp** ligand is lost. When **1** was dissolved in coordinating solvents, its characteristic bright orange color disappeared and was replaced by a yellow color. This color change occurred in methanol, acetone, and CH_3CN, but not in CH_2Cl_2. Since the bright orange color is characteristic of bis(phenanthroline) coordination to copper(I), it appeared that one of the ligands was displaced upon dissolution, even in a weakly coordinating solvent like acetone (Reaction 2, Y is solvent).

$$[Cu(\mathbf{dtbp})_2]^+ + Y \leftrightarrow [Cu(\mathbf{dtbp})(Y)]^+ + \mathbf{dtbp} \quad (2)$$

The binding affinity of the second **dtbp** ligand in **1** was determined by measuring a binding constant for Reaction 3. In CH_2Cl_2, [Cu(**dtbp**)(acetone)](SbF_6) was titrated with **dtbp**, and the growth of the MLCT absorption at 425 nm was monitored. The data were fit to an expression

(36) Arnold, D. R.; Baird, N. C.; Bolton, J. R.; Brand, J. C. D.; Jacobs, P. W. M.; DeMayo, P.; Ware, W. R. *Photochemistry: An Introduction*; Academic Press: New York, NY, 1974.

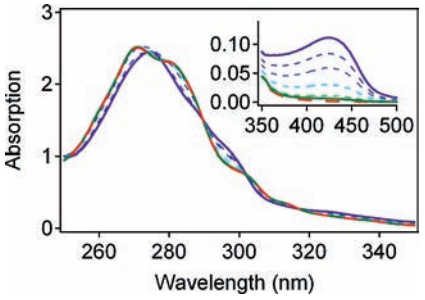

Figure 3. Reaction of **1** with CH_3CN followed by absorption spectroscopy. Electronic absorption spectra of **1** (36 μM in CH_2Cl_2) titrated with CH_3CN (0.2 equiv aliquots up to 1 equiv). The spectra obtained after addition of 0 (blue solid line), 1 (green solid line) and 3 (red dashed line) of CH_3CN are highlighted. Inset: the MLCT absorption of **1**.

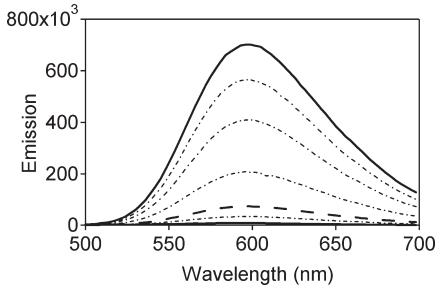

Figure 4. Reaction of **1** with CH_3CN followed by emission spectroscopy. Photoluminescence spectra of **1** (36 μM in CH_2Cl_2) titrated with CH_3CN (0.25 equiv aliquots up to 1 equiv). The spectra obtained after addition of 0 (solid line), 1 (dashed line) and 3 (dashed-dotted line) equiv of CH_3CN are highlighted. The excitation wavelength was 425 nm.

appropriate for complexes with high stability constants;[32] the resulting binding constant for **dtbp** was 9.9 (±0.3) × 10^5. This binding constant defines the relative affinities of acetone and **dtbp** for the Cu center, as it was not possible to prepare a complex bearing one **dtbp** and no other ligand.

$$[Cu(\mathbf{dtbp})(acetone)](SbF_6) + \mathbf{dtbp} \leftrightarrow [Cu(\mathbf{dtbp})_2](SbF_6) + acetone \quad (3)$$

Reactivity of 1 with CH_3CN. The reaction of **1** with CH_3CN was studied in more detail. Changes attributable to the displacement of **dtbp** from **1** were observed in the absorption and emission spectra of **1** upon titration with CH_3CN (Reaction 4, Figures 3 & 4). Most noteworthy was the loss of the MLCT absorption at 425 nm upon addition of 1 equiv of CH_3CN, and the appearance of new features between 300 and 325 nm (Figure 3). Changes in the $\pi \rightarrow \pi^*$ transition region were also observed. As CH_3CN was added, the 275 nm band split into two new bands: one at 271 nm, the position of the $\pi \rightarrow \pi^*$ absorption of the free **dtbp** ligand, and one at 279 nm. Independent synthesis and crystallographic[26] and spectroscopic characterization (Supporting Information, Figure S3) of $[Cu(\mathbf{dtbp})(NCCH_3)](PF_6)$ confirmed that the absorptions at 279, 310, and 325 nm were from the complex $[Cu(\mathbf{dtbp})(NCCH_3)]^+$. Addition of CH_3CN to **1** also resulted in loss of the MLCT-derived emission at 599 nm (Figure 4). Note that in both absorption and emission experiments spectral changes are observed up to 1 equiv of CH_3CN;

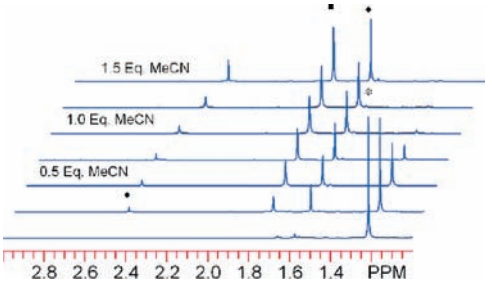

Figure 5. Reaction of **1** with CH_3CN followed by ^1H NMR. Shown are the changes in the aliphatic region upon titration of **1** with CH_3CN. Spectra proceed from bottom to top: **1** in CD_2Cl_2 was titrated with 0−1.5 equiv. of CH_3CN (in CD_2Cl_2) in 0.25 equivalent aliquots. The chemical shifts of the various *tert*-butyl protons of **dtbp** are indicated: **1** (*; δ 1.21 ppm), $[Cu(\mathbf{dtbp})(NCCH_3)]^+$ (♦; δ 1.55 ppm), and **dtbp** (■; δ 1. 73 ppm). The resonance that is initially observed at δ 2.43 ppm (●) is assigned to the methyl group of CH_3CN in $[Cu(\mathbf{dtbp})(NCCH_3)]^+$.

minimal further changes are observed upon addition of up to 3 equiv CH_3CN. The equilibrium constant for reaction 4, describing the relative binding affinities of CH_3CN and **dtbp**, was calculated to be 4 ($\pm$2) $\times$ 10^7.

$$[Cu(\mathbf{dtbp})_2]^+ + CH_3CN \leftrightarrow [Cu(\mathbf{dtbp})(CH_3CN)]^+ + \mathbf{dtbp} \quad (4)$$

The displacement of **dtbp** by CH_3CN was explicitly demonstrated by ^1H NMR (Figure 5), following changes in the distinct resonances of the *tert*-butyl substituents of **dtbp**. The *tert*-butyl groups of **1** appear at 1.21 ppm, the *tert*-butyl groups of the free **dtbp** ligand appear at 1.55 ppm, and those of the complex $[Cu(\mathbf{dtbp})(NCCH_3)]^+$ appear at 1.75 ppm (Supporting Information, Figure S4). As CH_3CN is added to **1**, the intensity of the resonance at 1.21 ppm decreases, and new resonances grow in simultaneously at 1.55 ppm and 1.73 ppm. This observation clearly reveals that CH_3CN displaces one **dtbp** ligand from the coordination sphere of copper(I). The reaction is essentially complete upon addition of 1 equiv CH_3CN. At 1 equiv, the 1.21 ppm resonance of **1** is barely observed. Minimal further change in the intensity of the resonances of free **dtbp** (1.55 ppm) and $[Cu(\mathbf{dtbp})(NCCH_3)]^+$ (1.73 ppm) occurs upon addition of up to 3 equiv CH_3CN. The methyl protons of CH_3CN appear at 2.43 ppm in $[Cu(\mathbf{dtbp})(NCCH_3)]^+$ as it is formed from **1** upon addition of 1 equiv CH_3CN. When excess CH_3CN is added, this resonance shifts toward that of free CH_3CN (2.04 ppm) suggesting that there is rapid exchange between the free and bound CH_3CN.

FT Raman analysis corroborates the displacement of a single **dtbp** ligand by CH_3CN (Figure 6). In the absence of CH_3CN, the Raman spectrum of **1** revealed a ligand-based ring vibration at 1391 cm^{-1}, with a shoulder at higher energy (Figure 6a). The analogous vibration appears at 1404 cm^{-1} in free **dtbp** and at 1420 cm^{-1} in $[Cu(\mathbf{dtbp})(NCCH_3)]^+$. As CH_3CN is added to **1**, the peak at 1391 cm^{-1} is replaced by two peaks, at the positions characteristic of the free ligand (1404 cm^{-1}) and $[Cu(\mathbf{dtbp})(NCCH_3)]^+$ (1421 cm^{-1}). The reaction can also be followed by the appearance of the C−N mode of bound CH_3CN in $[Cu(\mathbf{dtbp})(NCCH_3)]^+$ at 2283 cm^{-1}: this mode is completely absent in **1** and grows in only as CH_3CN is added. When 3 equiv of CH_3CN were added,

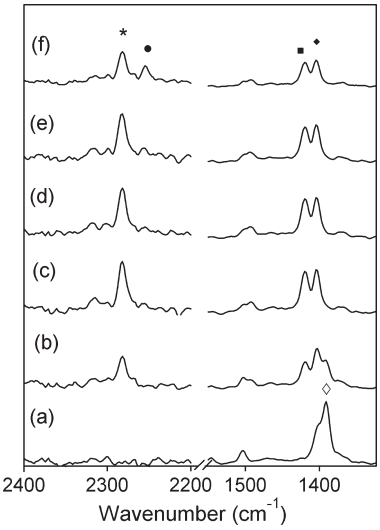

Figure 6. Titration of **1** with CH_3CN followed by FT-Raman spectroscopy. Spectra show the addition of (a) 0, (b) 0.5, (c) 1.0, (d) 1.5, (e) 2.0, and (f) 3.5 equiv. of CH_3CN to **1** in CH_2Cl_2 solution. Highlighted vibrations include: ν_{CN} of $[Cu(\mathbf{dtbp})(NCCH_3)]^+$ (*; 2283 cm^{-1}); ν_{CN} of free CH_3CN in CH_2Cl_2 solution (●; 2253 cm^{-1}); an a_1 vibration of free **dtbp** (♦; 1404 cm^{-1}), and analogous modes of **dtbp** in $[Cu(\mathbf{dtbp})(NCCH_3)]^+$ (■; 1424 cm^{-1}) and **dtbp** in **1** (◇; 1391 cm^{-1}).

an additional peak corresponding to free CH_3CN was observed at 2253 cm^{-1}. Notably, the ν_{C-N} of bound CH_3CN in $[Cu(\mathbf{dtbp})(NCCH_3)]^+$ is 30 cm^{-1} above the value of ν_{C-N} observed for free CH_3CN, indicating a non-classical interaction of copper(I) with CH_3CN in this complex.[37,38]

Reactivity of 1 with CO. CO displaces one **dtbp** ligand from **1** in a reaction analogous to that observed for CH_3CN (Reaction 5). The $[Cu(\mathbf{dtbp})(CO)]^+$ complex was independently synthesized from $[Cu(\mathbf{dtbp})(acetone)]^+$ and the characterization of this new complex will be discussed below as it pertains to the reactivity of **1**. Absorption, emission, FT Raman, and IR spectroscopies were used to monitor the reaction of **1** with excess CO; the spectroscopic features characteristic of **1** are replaced by those characteristic of $[Cu(\mathbf{dtbp})(CO)]^+$ and free **dtbp** upon reaction. A color change from bright orange to an almost-colorless pale yellow is observed as gaseous CO is added. This color change is complete within seconds. As in the reaction with CH_3CN, the MLCT absorption at 425 nm characteristic of **1** is lost, and the $\pi \rightarrow \pi^*$ transition at 275 nm is replaced by two new absorption features at 284 and 271 nm, due to $[Cu(\mathbf{dtbp})(CO)]^+$ and free **dtbp**, respectively (Supporting Information, Figure S5). Loss of the MLCT absorption band of **1** upon reaction with CO results in near complete loss of the MLCT-derived emission at 599 nm (Table 3). Also notable are changes in the ligand based ring vibrations in the FT Raman spectrum (Supporting Information, Figure S6), analogous to those observed in reaction with CH_3CN (Figure 6), with the appearance of a new C−O stretch at 2130 cm^{-1}.

$$[Cu(\mathbf{dtbp})_2]^+ + CO \leftrightarrow [Cu(\mathbf{dtbp})(CO)]^+ + \mathbf{dtbp} \quad (5)$$

The reaction of **1** with CO is reversible. When the solution obtained after reaction of **1** with CO, which

(37) Thomas, J. C.; Peters, J. C. *Polyhedron* **2004**, *23*, 2901–2913.
(38) Strauss, S. H. *Dalton Trans.* **2000**, 1–6.

Table 3. Excess CO and O_2 Reversibly Quench the Emission of **1**[a]

	percent initial emission ($I/I_0 \times 100$)	
	CO	O_2
1 in CH_2Cl_2	100%	100%
1st exposure	3.7%	44%
1st Ar sparge	87%	89%
2nd exposure	2.9%	42%
2nd Ar sparge	70%	83%

[a] A 36 μM solution of **1** in CH_2Cl_2 was exposed to excess CO or O_2. The gas was removed by sparging with Ar, and the solvent volume was restored. This procedure was repeated for a total of two times. Absorption (Supporting Information, Figures S5 and S9) and emission data were collected after each manipulation.

contained [Cu(**dtbp**)(CO)]$^+$ and free **dtbp**, was sparged with Ar, the characteristic absorption and emission features of **1** returned. When CO was reintroduced, the products [Cu(**dtbp**)(CO)]$^+$ and free **dtbp** were once again observed (Supporting Information, Figure S5). Exposing solutions of **1** to cycles of CO and Ar, with restoration of evaporated solvent, revealed that after two complete cycles (CO exposure, degassing with Ar, addition of lost solvent) 70% of the initial photoluminescence intensity was recovered (Table 3). Evidence of incomplete reversion is present in the absorption spectra (Supporting Information, Figure S5); the intensity of the MLCT absorption of **1** was not fully restored after addition and removal of CO. The reversibility of Reaction 5 was also studied by FT-IR. A series of spectra were recorded (1) before exposure of **1** to CO, (2) after bubbling with CO, and (3) after the reaction solution had been taken to dryness in vacuo and the resulting solid redissolved in fresh CH_2Cl_2. Figure 7 shows the ν_{C-O} stretching region of these spectra: no ν_{C-O} band was seen before exposure of **1** to CO (Figure 7a) but upon exposure of **1** to CO, a C−O stretch appeared at 2130 cm^1 (Figure 7b). When the products were dried in vacuo and redissolved in CH_2Cl_2, the C−O stretch disappeared from the spectrum (Figure 7c).

Reversible CO binding is only observed when a second **dtbp** ligand is present. FT-IR studies, parallel to those described for **1** above, were performed using the complex [Cu(**dtbp**)(acetone)](SbF$_6$). Excess CO reacted readily with [Cu(**dtbp**)(acetone)](SbF$_6$) to form [Cu(**dtbp**)(CO)]$^+$, as illustrated in Figure 7, spectra d and e. When the product [Cu(**dtbp**)(CO)]$^+$ was treated in the same manner as the product of the reaction of **1** with CO, that is, taken to dryness under vacuum and redissolved in fresh solvent, the CO remained bound to the metal center (Figure 7f). Excess **dtbp** ligand was then added to the same solution, the solvent was removed in vacuo, and the resulting solid was redissolved. The solution product in the presence of excess **dtbp** ligand bore no CO (Figure 7g). These experiments reveal that reversible CO binding is enabled by the presence of uncoordinated **dtbp**, which replaces CO as the ligand.

The complex [Cu(**dtbp**)(CO)]$^+$ was independently synthesized to corroborate the spectral assignments made in the reaction of **1** with CO. Reaction 6 was carried out in the non-coordinating solvent CH_2Cl_2 to prepare [Cu(**dtbp**)(CO)](SbF$_6$). Evaporation of the solvent under a CO flow was necessary to completely remove the acetone ligand, thus eliminating any competition for

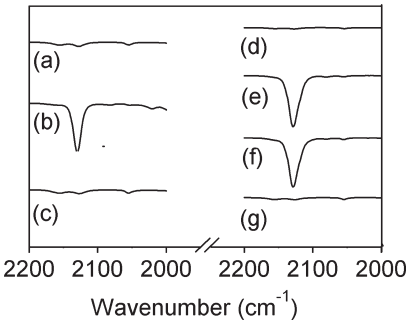

Figure 7. Reactions of **1** and [Cu(**dtbp**)(acetone)](SbF$_6$) with CO followed by solution FT-IR spectroscopy. Left column: FT-IR spectra of a solution of **1** in CH_2Cl_2: (a) in the absence of CO; (b) upon exposure to CO; (c) after removal of solvent in vacuo and addition of fresh solvent. Right column: FT-IR spectra of a solution of [Cu(**dtbp**)(acetone)](SbF$_6$) in CH_2Cl_2: (d) in the absence of CO; (e) upon exposure to CO; (f) after removal of solvent in vacuo and addition of fresh solvent; (g) the solution from (f) to which excess **dtbp** was added, the solvent was removed in vacuo, and fresh solvent was added.

ligation to the copper(I) center. As shown in Supporting Information, Figure S7, the IR spectrum of this complex in CH_2Cl_2 solution reveals a ν_{C-O} mode at 2130 cm^{-1}, illustrating classical binding of CO to copper(I).[38] The band at 2130 cm^{-1} shifts to 2080 cm^{-1} when the solution of [Cu(**dtbp**)(CO)]$^+$ is equilibrated with ^{13}CO, thus conclusively identifying this as the ν_{C-O} mode. The ^{1}H NMR spectrum of [Cu(**dtbp**)(CO)](SbF$_6$) showed no evidence of acetone methyl groups, and the *tert*-butyl methyl proton resonance is shifted downfield relative to that of [Cu(**dtbp**)(acetone)](SbF$_6$). The quaternary carbon of the CO ligand appeared at 173.24 ppm in the ^{13}C NMR spectrum.

$$[\mathrm{Cu}(\mathbf{dtbp})(\mathrm{acetone})](\mathrm{SbF_6}) + \mathrm{CO} \leftrightarrow [\mathrm{Cu}(\mathbf{dtbp})(\mathrm{CO})](\mathrm{SbF_6}) + \mathrm{acetone} \quad (6)$$

[Cu(**dtbp**)(CO)](SbF$_6$) crystallized in a centrosymmetric triclinic unit cell of $P\bar{1}$ symmetry containing two formula units ($Z = 2$), such that one [Cu(**dtbp**)(CO)]$^+$ cation and one SbF_6^- anion comprise the crystallographically independent part. The cation possesses pseudo-C_{2v} symmetry, with a trigonal planar three-coordinate Cu(I) (Figure 8). This complex is the first three-coordinate [Cu(**dtbp**)X]$^{+/0}$ complex in which the third ligand lies in the phenanthroline plane, in contrast to the distorted asymmetry of previously characterized [Cu(**dtbp**)X]$^{+/0}$ complexes.[26,39] The methyl groups of the *tert*-butyl substituents are positioned symmetrically so as to limit crowding about the CO ligand. The coordination sphere of the metal ion is composed of the two nitrogen atoms of the phenanthroline and the carbon atom of the CO ligand. The mean of 2.04 Å for the two pseudoequivalent Cu−N distances (2.045(2) Å, 2.034(3) Å) in the [Cu(**dtbp**)(CO)]$^+$ cation is similar to those of sterically unconstrained (2,9-phenanthroline)Cu(I) complexes, but 0.07 Å shorter than the mean Cu−N distance of 2.11 Å in sterically encumbered **1**.[26] A salient structural feature of [Cu(**dtbp**)(CO)]$^+$ is the linkage between the terminal CO and the d^{10} Cu(I) ion, with Cu−C and C−O bond

(39) Pallenberg, A. J.; Koenig, K. S.; Barnhart, D. M. *Inorg. Chem.* **1995**, *34*, 2833–2840.

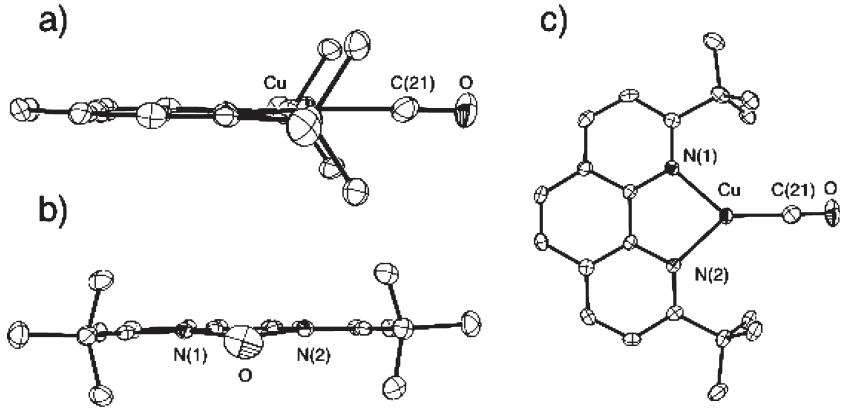

Figure 8. Molecular drawings of the cation in [Cu(**dtbp**)(CO)](SbF_6) shown with 50% probability thermal ellipsoids. The Cu atom and the CO ligand are perfectly in the plane of the phenanthroline ligand. H atoms have been omitted for clarity. Three views are shown: (a) side view, (b) end view, and (c) top view.

distances of 1.814(3) Å and 1.132(3) Å, respectively. Notably, the C−O bond is only slightly longer than the 1.128 Å of free CO, which in conjunction with the high C−O stretching frequency reveal the minimal back bonding in this complex.

Reactivity of 1 with O_2. Dioxygen does not displace **dtbp** from **1** (Reaction 7), but O_2 does partially quench the luminescence of **1**. Upon exposure to excess O_2 the absorption spectrum of **1** changes slightly; a minor diminution of the intensity of the $\pi\rightarrow\pi^*$ ligand absorption (275 nm) is observed (Supporting Information, Figure S8). There is no evidence of an absorption band at 271 nm from the free ligand or of any other new bands. Similarly, there is a modest change in the intensity of the MLCT absorption of **1** upon O_2 addition. Since the MLCT-derived emission intensity is very sensitive to the presence of the second **dtbp** ligand, we conclude that O_2 does not displace **dtbp** from **1**. Excess O_2 does quench the luminescence of **1**, albeit to a substantially lesser extent than excess CO (Table 3). The luminescence quenching observed on exposure of **1** to O_2 is reversible upon sparging the solution with Ar. The quenching induced by O_2 is more reversible than that induced by CO; after two exposures of **1** to O_2, each followed by removal with an Ar sparge, 83% of the initial emission intensity is restored.

$$[Cu(\mathbf{dtbp})_2]^+ + O_2 \leftrightarrow \text{No Reaction} \qquad (7)$$

Reactivity of 1 with CH_3NC. CH_3NC displaces both **dtbp** ligands from **1** (Reactions 8a,b). As was observed for reaction of **1** with CH_3CN and CO, addition of 1 equiv CH_3NC is accompanied by changes in the absorption spectrum consistent with displacement of one **dtbp** ligand from the metal (Figure 9). However, unlike CH_3CN or CO, addition of CH_3NC beyond 1 equiv results in a continued increase in the absorption at 271 nm corresponding to free **dtbp**, indicating that CH_3NC is capable of displacing the second **dtbp**. Equilibrium constants for reactions 8a and 8b were calculated from the absorption data. The binding constant for the first CH_3NC (Reaction 8a) was found to be 3×10^9 using the intensity at 425 nm from 0 to 1 equiv CH_3NC.

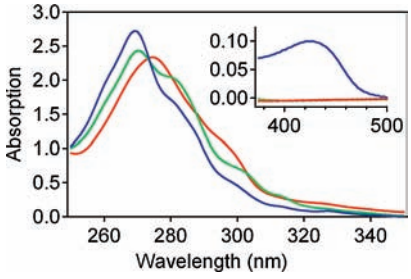

Figure 9. Reaction of **1** with CH_3NC followed by absorption spectroscopy. Electronic absorption spectra of **1** (36 μM in CH_2Cl_2) titrated with CH_3NC. The spectra obtained after addition of 0 (red solid line), 1 (green solid line) and 6 (blue solid line) equiv of CH_3NC are shown. Inset: the MLCT absorption of **1**.

The binding constant for the additional CH_3NC ligands (Reaction 8b) was calculated to be 4×10^3 using intensities at 269 nm from 1 to 6 equiv CH_3NC. The identity of the final copper(I) product of reaction 8b was not verified but is believed to be a homoleptic isonitrile complex, analogous to the common copper(I) starting material $[Cu(CH_3CN)_4]^+$. Thus, the sum of Reactions 8a and 8b, which is Reaction 8c, exhibits an equilibrium constant of 1.2×10^{13} M^{-2}.

$$[Cu(\mathbf{dtbp})_2]^+ + CH_3NC \leftrightarrow [Cu(\mathbf{dtbp})(CH_3NC)]^+ + \mathbf{dtbp} \qquad (8a)$$

$$[Cu(\mathbf{dtbp})(CH_3NC)]^+ + 3CH_3NC + \mathbf{dtbp} \leftrightarrow [Cu(CH_3NC)_4]^+ + 2\mathbf{dtbp} \qquad (8b)$$

$$[Cu(\mathbf{dtbp})_2]^+ + 4CH_3NC \leftrightarrow [Cu(CH_3NC)_4]^+ + 2\mathbf{dtbp} \qquad (8c)$$

Discussion

The properties of **1** extend established trends in absorption and emission characteristics of bis(phenanthroline)copper(I) complexes.[5,6,8,9] Table 1 lists photophysical characteristics of selected complexes with varied substituents at the 2 and 9

positions of the ligand and organized in order of decreasing emission lifetime and decreasing quantum yield. The lifetime and quantum yield correlate with the apparent steric bulk of the ligand, with complex **1** showing the longest observed lifetime and highest quantum yield in this class of complexes. The lifetime increases with the energy of emission in keeping with the energy gap law.[29] The presence of the bulky *tert*-butyl groups in complex **1** modestly increases the radiative relaxation rate, k_r, and dramatically decreases the nonradiative relaxation rate, k_{nr}. This substantial decrease in k_{nr} is consistent with inhibition of the geometric reorganization in the excited state, as complexes in which the tetrahedral-to-square planar structural change is inhibited are consistently more emissive.[5,6,8,9] Further evidence for minimal reorganization in the excited state is provided by the difference between the energies of absorption and emission, whose value is smaller for **1** than for other $[Cu(R_2Phen)_2]^+$ complexes. Luminescence in complexes with MLCT-derived excited states may occur from states of singlet or triplet multiplicity, and the magnitude of $E_{Abs} - E_{Em}$ is related to the energy losses that occur with internal conversion, intersystem crossing, and geometric reorganization.[40,41] The 0.847 eV difference observed in **1** implies that there are smaller energy losses, presumably because the bulky *tert*-butyl groups minimize structural changes in the excited states. The oscillator strength of the complex **1** MLCT absorption, with an ε of 3100 L M^{-1} cm^{-1}, is among the smallest of this series because of the poorer overlap between the metal and ligand orbitals that is a consequence of the elongated Cu−N bonds.[26]

Differential effects of sterics and electronics on the properties of $[Cu(R_2Phen)_2]^+$ complexes may be deduced from a comparison between **1** and $[Cu(bfp)_2]^+$.[42,43] The last three entries of Table 1 feature ligands with electron withdrawing groups at the 2 and 9 positions, for which there is no obvious correlation between the photophysical properties and electronic effects. We note that $[Cu(bfp)_2]^+$, with the most electron withdrawing ligands, exhibits a value of $E_{Abs} - E_{Em}$ that is smaller than that of complex **1**. One might conclude that $[Cu(bfp)_2]^+$ exhibits less excited-state distortion than **1**; however, the ground-state crystallographic data show that $[Cu(bfp)_2]^+$ is in fact more easily distorted.[43] The data thus suggest that the behavior of $[Cu(bfp)_2]^+$ is largely dictated by electronic, not steric, effects. This conclusion is supported by a comparison of the electrochemical behavior of $[Cu(bfp)_2]^+$ and **1**. Both complexes exhibit high positive ground-state reduction potentials. The electrochemical behavior of $[Cu(bfp)_2]^+$ is perfectly reversible, and the potential is the most positive among all $[Cu(R_2Phen)_2]^+$ complexes (Table 2), as the highly electron withdrawing groups stabilize the copper(I) state.[42] The apparent $E_{1/2}$ for complex **1** is the most positive among complexes with 2,9-dialkyl-1,10-phenanthroline ligands, illustrated by the first four entries in Table 2. The reduction potential increases with steric bulk, which stabilizes copper(I) relative to copper(II) by inhibition of the geometric reorganization required in the latter.[9] In contrast to $[Cu(bfp)_2]^+$, the electrochemical behavior of **1** is not reversible. With modestly sized CF_3 substituents, $[Cu(bfp)_2]^+$ is able to accommodate the tetragonal geometry preferred by copper(II),[43] while the exceptional bulk of the *tert*-butyl groups renders the oxidized form of complex **1** unstable. Also listed in Table 2 are the excited-state reduction potentials for the $[Cu^{2+}(R_2Phen)(R_2Phen^{-\bullet})]|[Cu^{2+}(R_2Phen)_2]$ couple. We note that the high ΔG_{es} of complex **1** contributes a large negative value in the calculation of the excited-state reduction potential, and the calculated potential indicates that the excited state of **1**, $[Cu^{2+}(\mathbf{dtbp})(\mathbf{dtbp}^{-\bullet})]$, is a potent photoreductant. In contrast, the highly positive reduction potential of $[Cu(bfp)_2]^+$ coupled with a much lower ΔG_{es} value renders $[Cu^{2+}(bfp)(bfp^{-\bullet})]$ a weak photoreductant.[42]

Copper(I) complexes are generally labile; however, the exceptionally bulky *tert*-butyl substituents at the 2 and 9 positions of the phenanthroline enable unique ligand substitution reactivity in complex **1**. In coordinating solvents, such as acetone or acetonitrile, one of the bidentate **dtbp** ligands is replaced by solvent. For most complexes in this family, the only observable species in solution is the bis-phenanthroline species, $[Cu(R_2Phen)_2]^+$, because of the chelating nature of the ligands.[39] However, the **dtbp** ligand is so bulky that accommodating four *tert*-butyl groups about the copper(I) center is more challenging, and only the novel reaction conditions under which complex **1** is synthesized allow for the binding of two **dtbp** ligands.[26,44] Complex **1** is prepared in acetone by reaction of 2 equiv of **dtbp** with 1 equiv of $Ag[B(C_6F_5)_4]$ and excess copper metal. With an excess of acetone present, the immediate product is the acetone solvato complex, $[Cu(\mathbf{dtbp})(acetone)]^+$. When the acetone solvent is removed upon workup, the second equivalent of **dtbp** binds to form complex **1**. Spectrophotometric titration of the acetone solvato complex with the second **dtbp** to form **1** revealed that the binding constant of **dtbp** relative to the bound acetone was 9.9 ($\pm$0.3) $\times$ 10^5. In stark contrast, titration of 1 equiv of CH_3CN into complex **1** revealed the binding constant of CH_3CN relative to the second **dtbp** ligand to be 4 ($\pm$2) $\times$ 10^7. These binding affinities dramatically demonstrate that a ligand displacement reaction on $[Cu(CH_3CN)_4]^+$, in which a minimum 4 equiv of CH_3CN are present regardless of solvent, is a poor choice for the synthesis of complex **1**.[20,26]

An important consequence of low affinity for the second **dtbp** ligand is its facile displacement in solution. The solid-state and solution-state FT-Raman spectra of complex **1** revealed differences in the intense feature, which we assign to an a_1 symmetry phenanthroline ring vibration.[45] The solid-state spectrum of **1** reveals a peak at 1400 cm^{-1}, while the solution-state spectrum in CH_2Cl_2 reveals two frequencies associated with this feature: a peak at 1391 cm^{-1}, with a higher energy shoulder at 1402 cm^{-1} (Supporting Information, Figures S9 and S10). The single peak in the solid-state spectrum indicates an equality in the binding of the two **dtbp** ligands about the copper(I) center, confirming what is observed crystallographically where the Cu−N distances are similar.[26] In contrast, the two peaks of the solution-state

(40) Iwamura, M.; Takeuchi, S.; Tahara, T. *J. Am. Chem. Soc.* **2007**, *129*, 5248–5256.
(41) Bock, C. R.; Connor, J. A.; Gutierrez, A. R.; Meyer, T. J.; Whitten, D. G.; Sullivan, B. P.; Nagle, J. K. *J. Am. Chem. Soc.* **1979**, *101*, 4815–4824.
(42) Miller, M. T.; Gantzel, P. K.; Karpishin, T. B. *Angew. Chem., Int. Ed.* **1998**, *37*, 1556–1558.
(43) Kovalevsky, A. Y.; Gembicky, M.; Coppens, P. *Inorg. Chem.* **2004**, *43*, 8282–8289.
(44) Morgan, H. H. *J. Chem. Soc.* **1923**, 2901–2907.
(45) Reiher, M.; Brehm, G.; Schneider, S. *J. Phys. Chem. A* **2004**, *108*, 734–742.

spectrum suggest an inequality in the binding of the two phenanthroline ligands about the metal center. The position of the shoulder, 1402 cm^{-1}, is within 2 cm^{-1} of the a_1 vibration observed in a CH_2Cl_2 solution of free **dtbp**, 1404 cm^{-1} (Supporting Information, Figure S6e). The higher energy shoulder suggests the presence of a population of weakly associated **dtbp** in solution that arises as a result of the increased steric congestion about the copper(I) center. These data also suggest that while the two **dtbp** ligands of complex **1** are bound in similar fashion in the solid state (1400 cm^{-1}), the solid-state binding is more similar to that of the weakly bound **dtbp** of **1** in solution (1402 cm^{-1}) than to that of the strongly bound **dtbp** (1391 cm^{-1}).

The intrinsic instability of the homoleptic complex **1** may be of value in the design of molecular-based devices, as labile copper(I) complexes have been exploited to great effect in the synthesis of controlled molecular assemblies.[46−51] In particular, the coordination geometry and coordination number preferences of copper(I), and the distinctly different preferences of copper(II), have been used in the design of photo- or electrochemically addressable molecular machines.[52] Bulky copper(I) phenanthroline complexes have proved particularly useful in the synthesis of predictable assemblies of heteroleptic complexes in which it is essential to control the thermodynamics.[53−55] This HETPHEN approach is characterized by judicious choice of bulky phenanthroline ligands, such that the two homoleptic $[Cu(R_2Phen)_2]^+$ species are less stable than the heteroleptic combination. This method has exploited bulky aryl-substituted phenanthroline ligands; however, the instability of complex **1** suggests that *tert*-butyl-phenanthroline may also be useful for this purpose. The synthetic method used to prepare **1**,[26] which avoids $[Cu(CH_3CN)_4]^+$ as a starting material, was superior for the preparation of the heteroleptic complex [Cu(dmp)(**dtbp**)]$^+$,[20] and this method may be similarly advantageous in the clean preparation of more complex heteroleptic assemblies.

The excellent photophysical properties of complex **1** and its instability toward ligand substitution set the stage for the exploitation of this complex in sensing applications. For example, CO has a greater binding affinity for the copper ion than does the second bidentate **dtbp** ligand, and the binding of CO results in near complete quenching of luminescence. The excess **dtbp** remaining in solution aids in driving off the bound CO, reversing the reaction and restoring the luminescence. This facile reversibility is only possible in the presence of the extra equivalent of **dtbp** to fill the coordination sphere of the copper ion. Reversible luminescence quenching is also observed with O_2; however, the absence of any change in the absorption spectrum was inconsistent with a ligand exchange reaction. Rather, the data suggest an outer-sphere interaction between between **1** and O_2, similar to that observed previously for [Cu(dmp)(**dtbp**)]$^+$.[56] Interestingly, complex **1** shows virtually no tendency to react with O_2,[57,58] which is unusual for copper(I) complexes but consistent with the large positive reduction potential that inhibits oxidative reactivity.

Using the qualitative and quantitative data collected in this study, we may construct a ligand affinity series for the $[Cu(\mathbf{dtbp})]^+$ fragment. The binding affinity for an additional ligand increases in the following order: acetone < **dtbp** < CO $\approx$ CH_3CN < CH_3NC. Strongly donating monodentate ligands, CO, CH_3CN and CH_3NC, react with **1** to displace one bidentate **dtbp** ligand. This reactivity is unique in that it defies the chelate effect, in which bidentate ligands typically enhance the stability of metal complexes relative to monodentate ligands. Furthermore, in the case of CO and CH_3CN, the greater affinity of the monodentate ligands over the bidentate **dtbp** is observed in the absence of significant backbonding between the copper(I) and π acid ligand.[38] CH_3NC very efficiently displaces the first **dtbp** ligand from complex **1**, and also displaces the remaining bound **dtbp** ligand, although considerably less efficiently.

Conclusion

We have characterized the photophysical properties of the most sterically constrained copper(I)-phenanthroline complex, $[Cu(\mathbf{dtbp})_2]^+$. The photophysical measurements revealed a quantum yield on par with and an excited-state lifetime longer than those of $[Ru(bpy)_3]^{2+}$. The exceptional steric constraints in complex **1** weaken the metal−ligand bonding, which in turn afforded a unique type of reactivity. One of the chelating **dtbp** ligands is readily replaced by strongly donating, monodentate ligands such as acetonitrile and CO. The unique combination of excellent photophysical properties and ligand displacement reactivity renders complex **1** attractive for use in sensors, molecular machines, or photoelectronic devices.

Acknowledgment. The authors are grateful to Dr. Ewald Terpetschnig of ISS Inc. for the emission lifetime measurements. We would also like to thank Dr. Umesh Agarwal and Mr. Richard Reiner of the Forest Products Laboratory (Madison, WI) for use of the FT-Raman spectrometer. Acknowledgment is made to the Donors of the American Chemical Society Petroleum Research Fund for support of this research (ACS-PRF Grant 42041-AC3 to J.N.B.).

Supporting Information Available: Electronic absorption and NMR spectra of $[Cu(\mathbf{dtbp})NCCH_3]PF_6$. Cyclic voltammogram of **1**, and comparison of corrected emission spectrum to that of

(46) Dietrich-Buchecker, C. O.; Sauvage, J. P. *Chem. Rev.* **1987**, *87* 795–810.
(47) Sauvage, J. P. *Acc. Chem. Res.* **1990**, *23*, 319–327.
(48) Collin, J.-P.; Dietrich-Buchecker, C.; Gavina, P.; Jimenez-Molero, M. C.; Sauvage, J.-P. *Acc. Chem. Res.* **2001**, *34*, 477–487.
(49) Dietrich-Buchecker, C.; Jimenez-Molero, M. C.; Sartor, V.; Sauvage, J.-P. *Pure Appl. Chem.* **2003**, *75*, 1383–1393.
(50) Nitschke, J. R. *Acc. Chem. Res.* **2007**, *40*, 103–112.
(51) Schultz, D.; Nitschke, J. R. *Proc. Natl. Acad. Sci. U.S.A.* **2005**, *102*, 11191–11195.
(52) Livoreil, A.; Sauvage, J.-P.; Armaroli, N.; Balzani, V.; Flamigni, L.; Ventura, B. *J. Am. Chem. Soc.* **1997**, *119*, 12114–12124.
(53) Schmittel, M.; Ganz, A. *Chem. Commun.* **1997**, 999–1000.
(54) Schmittel, M.; Michel, C.; Liu, S.-X.; Schildbach, D.; Fenske, D. *Eur. J. Inorg. Chem.* **2001**, 1155–1166.
(55) Kalsani, V.; Bodenstedt, H.; Fenske, D.; Schmittel, M. *Eur. J. Inorg. Chem.* **2005**, 1841–1849.
(56) Miller, M. T.; Karpishin, T. B. *Sens. Actuators, B* **1999**, *B61*, 222–224.
(57) Lewis, E. A.; Tolman, W. B. *Chem. Rev.* **2004**, *104*, 1047–1076.
(58) Mirica, L. M.; Ottenwaelder, X.; Stack, T. D. P. *Chem. Rev.* **2004**, *104*, 1013–1045.
(59) Juris, A.; Balzani, V.; Barigelletti, F.; Campagna, S.; Belser, P. Von Zelewsky, A. *Coord. Chem. Rev.* **1988**, *84*, 85–277.
(60) Cunningham, K. L.; McMillin, D. R. *Inorg. Chem.* **1998**, *37* 4114–4119.

[Cu(**dtbp**)(dmp)]BF_4. The reaction of **1** with CO followed by electronic absorption, FT-Raman and FT-IR spectroscopy, and FT Raman band assignments. This material is available free of charge via the Internet at http://pubs.acs.org. Crystallographic data collection parameters, atomic coordinates, bond parameters, and spectral parameters for [Cu(**dtbp**)CO]SbF_6. CCDC 724725 contains the supplementary crystallographic data; these data may be obtained free of charge from The Cambridge Crystallographic Data Centre via www.ccdc.cam.ac.uk/data_request/cif.